https://doi.org/10.5194/wes-2023-91
Preprint. Discussion started: 16 August 2023
© Author(s) 2023. CC BY 4.0 License.

Fractal-based numerical simulation of multivariate typhoon wind speeds utilizing Weierstrass Mandelbrot function

Kang Cai[1], Mingfeng Huang[2], Qiang Li[3], Qing Wang[4], Yong Chen[5], Lizhong Wang[6]

[1]Institute of Structural Engineering, College of Civil Engineering and Architecture, Zhejiang Univ., Hangzhou 310058, P.R. China. Center for Balance Architecture, Zhejiang Univ., Hangzhou 310058, P.R. China.

[2]Institute of Structural Engineering, College of Civil Engineering and Architecture, Zhejiang Univ., Hangzhou 310058, P.R. China; Center for Balance Architecture, Zhejiang Univ., Hangzhou 310058, P.R. China.

[3]School of Civil Engineering and Architecture, NingboTech Univ., Ningbo 315100, P.R. China; Ningbo Research Institute, Zhejiang Univ., Ningbo 315100, P.R. China.

[4]Zhejiang Huadong Mapping and Engineering Safety Technology co., Ltd, Hangzhou 310014, P.R. China.

[5]Institute of Structural Engineering, College of Civil Engineering and Architecture, Zhejiang Univ., Hangzhou 310058, P.R. China.

[6]College of Ocean Engineering, Zhejiang University, Zhoushan 316000, P.R. China.

Correspondence to: Mingfeng Huang (mfhuang@zju.edu.cn)

Abstract: This paper proposes a fractal-based technique for simulating multivariate nonstationary wind speed fields by the stochastic Weierstrass Mandelbrot function. Upon conducting a systematic fractal analysis, it was found that the structure function method is more suitable and reliable than the box counting method, variation method, and R/S analysis method for estimating the fractal dimension of the stochastic wind speed series. Wind field measurement at the meteorological gradient tower with a height of 356 m in Shenzhen was conducted during Typhoon Mangkhut (2018). Significant non-stationary properties and fractal dimensions of typhoon wind speed data at various heights were analyzed and used to demonstrate the effectiveness of the proposed multivariate typhoon wind speed simulation method. The multivariate wind speed components simulated by the proposed fractal-based method are in good agreement with the measured records in terms of the fractal dimension, standard deviation, probability density function, wind spectrum and cross-correlation coefficient.

https://doi.org/10.5194/wes-2023-91
Preprint. Discussion started: 16 August 2023
© Author(s) 2023. CC BY 4.0 License.

Keywords: Fractal dimension; Structure function method; Simulation of multivariate nonstationary wind speeds; Weierstrass Mandelbrot function;

1 Introduction

Many patterns observed in nature, i.e. snowflake, involve invisible recurrent layers that are connected through a scaling factor, resulting in self-similarity across different scales. This creates a cascade of activity that repeats at smaller scales (Shlesinger, 1990). Processes with this feature were regarded as fractals (Mandelbrot, 1983, 1994). It is worth noting that fractals focus on the representation of complex physical systems that cannot be appropriately demonstrated in the framework of Euclidean terms. The fractal dimension, which quantifies the degree of self-similarity in natural processes, is a fundamental parameter for investigating the underlying simplicity in the organization of these processes (Rubalcaba, 1997).

The fractal dimensional analysis on wind speed time series has received increasing attention (Sakamoto et al., 2007; Chang et al., 2012; Fortuna et al., 2014; Harrouni, 2013, 2018; Cadenas et al., 2019). At present, there are several algorithms available for estimating the fractal dimension of a given wind speed time series, including the box counting method (Sarkar and Chaudhuri, 1994; Breslin and Belward, 1999; Fortuna et al., 2014; Cadenas et al., 2019; Shu et al., 2021), variation method (Dubuc et al., 1987; Syu and Kirchhoff, 1993), R/S analysis method (Peters, 1991; Zhong et al, 2012; Jiang et al., 2017), and structure function method (Ganti and Bhushan, 1995; Zhong et al, 2012; Wang and Xiang, 2013). Syu and Kirchhoff (1993) employed the variation method to obtain a fractal dimension of 1.60±0.03 for six different wind speed records from Altamont. Li et al (2001) calculated the fractal

https://doi.org/10.5194/wes-2023-91
Preprint. Discussion started: 16 August 2023
© Author(s) 2023. CC BY 4.0 License.

dimension of the high-frequency part of the wind turbulence signal using the variation method and found that it had a fixed dimension of 1.7 in average, which indicates a clear self-similarity feature of the wind speed time history record. Sakamoto et al (2007) applied the Higuchi method (Higuchi, 1988) and obtained the fractal dimensions, i.e., 2, 1.9 and 1.7 for the upwind, easterly and northerly winds, respectively. Chang et al. (2012) found that the annual mean fractal dimension values extracted by the box counting method ranged between 1.61 and 1.66. Tijera et al. (2012) observed that the fractal dimensions of horizontal and vertical velocity fluctuations at different heights (5.8 m, 13.5 m, and 32 m) using the box counting method ranged from 1.30 to nearly 1.00. Harrouni (2013) used the rectangular coverage method to collect the fractal dimension of daily wind speed series and found that the average dimension for one year was 1.92. Fortuna et al. (2014) reported average fractal dimension values of 1.19 and 1.41 for daily and hourly mean wind speeds, respectively, using mono-fractal, multi-fractal, and power spectra approaches. It is evident that the estimation of the fractal dimension of the wind speed records shows significant discrepancy due to the different methods used. Therefore, there is a pressing need to find a suitable method for estimating fractal dimensions in practical applications, and it is necessary to conduct a detailed comparative analysis of methods for fractal dimension estimation.

Additionally, generating wind speed time series numerically is a topic of great interest in many engineering applications, such as structural dynamic analysis, reliability estimation, fragility analysis and resilience assessment in structural wind engineering design (Huang et al. 2020). Various methods for generating time series of wind speed have been proposed, including the harmonic superimposing method (HSM) (Shinozuka and Jan, 1972), linear filtering method (Mignoler and Spanos, 1987), fuzzy set theory (Zhu et al., 2011), neural network techniques (Olaofe, 2014), support vector machines (Liu et al., 2014), Kalman filtering method (Chen et al., 2014), and time-mapping technique (Yassin et al., 2023). In wind engineering field, HSM has been widely used due to its simplicity and effectiveness. It is noteworthy that these methods were developed by modelling the intrinsic characteristics of turbulent wind (Shinozuka and Jan 1972; Yassin et al. 2023) or employing new kind of regression methods (Mignoler and Spanos 1987; Chen et al. 2014). However, none of them could fully capture the fractal characteristics of wind speed time series. Therefore, further research is needed to explore wind speed simulation methods that incorporate fractal characteristics. For this purpose, the Weierstrass Mandelbrot (WM) fractal function method is a suitable candidate, as it has been increasingly studied and utilized to simulate fractal surface profiles due to its ability to describe the fractal characteristics of time series (Berry and Lewis, 1980; Majumdar et al., 1990,1991; Ganti and Bhushan, 1995; Wang and Xiang, 2013). Humphrey et al. (1992) used the deterministic multi-fractal WM function with fractal dimensions of 1.95 and 1.62 to simulate the turbulent velocity records in the case of high-speed flow over an obstruction. Barszcz et al. (2012) developed a wind speed modelling method based on a deterministic WM function. Due to the randomness of wind, stochastic WM functions are more appropriate for simulating turbulent wind speed time series than the deterministic WM functions. Liu et al. (2013) discussed the use of stochastic WM function to simulate fractal wind fluctuations with a constant fractal dimension of 1.7. Wu et al. (2015) employed the stochastic WM function to simulate fluctuating wind speeds, and compared the results to the observed wind speed data in terms of fractal dimension, probability distribution, power spectrum, and cross-correlation coefficients. Lyu et al. (2018) proposed a combined simulation method based on weighted amplitude wave superposition and

https://doi.org/10.5194/wes-2023-91
Preprint. Discussion started: 16 August 2023
© Author(s) 2023. CC BY 4.0 License.

stochastic WM function, but with a fixed fractal dimension of 1.7. Since the fractal dimension of wind speed time series can vary with different wind conditions, it is recommended in this work to employ stochastic WM functions with varying fractal dimensions for numerical simulation of wind speed time series. Furthermore, natural winds may not satisfy the stationary assumption when dealing with wind speed data during extreme weather conditions, i.e., typhoon, thunderstorms or tornadoes (Cai et al. 2022). The current fractal-based simulation method is lack of ability to capture the nonstationary feature of wind speeds. In this paper, a new fractal-based numerical simulation method is developed for generating multivariate nonstationary typhoon wind speeds.

The paper is organized as follows: Section 2 firstly discusses the fractal-dimension estimation methods, then the stochastic WM function-based numerical simulation method (SWM method) is proposed for synthesizing multivariate nonstationary typhoon wind speeds. Section 3.1 provides details on the wind speed data collected during Typhoon Mangkhut. Section 3.2 compares the fractal dimensions estimated by various methods for typhoon wind speed data recorded at different heights. Section 3.3 presents the numerical simulation results of typhoon wind speeds using the proposed fractal-based SWM method. Finally, some concluding remarks are provided in Section 4.

2 Methodology

2.1 Fractal Analysis

This section aims to compare the following four commonly used methods, i.e., the box counting method, variation method, R/S analysis method and structure function method, based on their performance in estimating fractal dimension of the stochastic WM functions. Its goal is to identify and

https://doi.org/10.5194/wes-2023-91
Preprint. Discussion started: 16 August 2023
© Author(s) 2023. CC BY 4.0 License.

recommend the most appropriate fractal dimension estimation method for wind speed data.

2.1.1 Methods for estimating fractal dimensions of wind speed series

The box counting method mainly consists of placing the wind speed time series with grids, and then counting the number of non-overlapping boxes completely covering the time series. The relationship between the number of boxes, $N(L)$, and the width of the box, L, can be given by

$$N(L) \propto L^{-D} \tag{1}$$

The dimension D can be computed by the least-square fit of the curve $\log_2(N(L))$ versus $\log_2(1/L)$.

The variation method was originally proposed by Dubuc et al (1987) as a means of estimating the fractal dimension of rough surfaces. Given a wind speed time series $u(x)$, boxes with a bottom edge length of 2ϵ are used to cover the series. The side edge of the box $v(x,\epsilon)$ is defined by

$$v(x,\epsilon) = sup\, u(x') - inf\, u(x'), \qquad x' \in [x-\epsilon, x+\epsilon] \tag{2}$$

The ϵ variation $V(\epsilon,u)$ of wind speed $u(x)$ is then calculated as the sum of the areas of all the boxes, given by

$$V(\epsilon,u) = \sum v(x,\epsilon)\cdot 2\epsilon \tag{3}$$

The fractal dimension D will be obtained from the least square line passing through the points $(\log_2(1/\epsilon), \log_2(V(\epsilon,u)/\epsilon^2))$. The detailed procedures were presented in the reference by Syu and Kirchhoff (1993).

For the purpose of determining the fractal dimension, the R/S analysis method employs the following measures. At a given scale n, the mean value is calculated by

$$\bar{u}_n = \frac{1}{n}\sum_{x=1}^{n} u(x) \tag{4}$$

and the total accumulative deviation is given by

https://doi.org/10.5194/wes-2023-91
Preprint. Discussion started: 16 August 2023
© Author(s) 2023. CC BY 4.0 License.

$$u(x,n) = \sum_{x=1}^{n} [u(x) - \bar{u}_n] \tag{5}$$

The extreme difference, $R(n)$, is obtained as

$$R(n) = \max_{1 \le x \ll n} u(x,n) - \min_{1 \le x \ll n} u(x,n) \tag{6}$$

Additionally, the standard deviation is

$$S(n) = \sqrt{\frac{1}{n} \sum_{x=1}^{n} [u(x) - \bar{u}_n]^2} \tag{7}$$

Using the relationship $R(n)/S(n) \propto n^H$ (Peters, 1991), the Hurst exponent H could be obtained by linear fitting between the values $\log_2(n)$ and $\log_2(R(n)/S(n))$, and the fractal dimension is then given by D=2-H (Rehman and Siddiqi, 2009).

The structure function of order p was defined as

$$S_p(r) = \frac{1}{L-r} \int_0^{L-r} \{u(x+r) - u(x)\}^p dx, \tag{8}$$

where r is called the interval scale, which was originally introduced to describe the fine structure of turbulence in fluid mechanics (e.g., Shivamoggi, 1995; Arenas and Chorin, 2006)). Later, it became a popular tool for investigating surface roughness (e.g., Ganti and Bhushan, 1995). Notably, the order-2 structure function, $S(r)$, is closely related to the autocovariance function, R, through $S(r)=2\{R(0)-R(r)\}$, and includes the same information as R and its power spectral density function, but provides more practical merit (Thomas et al, 1999). For a fractal profile, the $S(r)$ is a function of the fractal dimension D, with

$$S(r) \propto r^{4-2D} \tag{9}$$

After plotting the $\log_2(r)$ versus the value $\log_2(S(r))$ and fitting a line to the plot curve, the fractal dimension is obtained by $D = (4 - \mathrm{K})/2$, where the K is the slope of the fitted line. The more detailed

https://doi.org/10.5194/wes-2023-91
Preprint. Discussion started: 16 August 2023
© Author(s) 2023. CC BY 4.0 License.

process could be found in Thomas et al (1999) and Zhong et al (2012).

For a pure random sequence, it is easy to get that the structure function almost keeps constant for each interval scale. This results in a zero slope of the fitted line, indicating a fractal dimension of 2 for the concerned random sequence. On the other hand, if the series very slowly over time, the fractal dimension is close to unit with a constant slope of K=2.

2.1.2 Comparison of the fractal dimension estimation methods based on the WM function

To determine the most appropriate method for estimating the fractal dimension of wind speeds, it is necessary to introduce the WM function with the known fractal dimension D. Notably, the WM function is continuous but non-differentiable at all points and possesses no scale (Berry and Lewis, 1980), as follows

$$W(t) = \sum_{n(l)=-\infty}^{\infty} \frac{(1-e^{i\gamma^{n(l)}t})e^{i\emptyset(l)}}{\gamma^{(2-D)\cdot n(l)}} \quad (1 < D < 2, \gamma > 1, \emptyset = arbitrary\ phases) \qquad (10)$$

where D represents the fractal dimension of the graph of $W(t)$; The frequencies γ^n form a 'Weierstrass spectrum', spanning the range from zero to infinity; The phases $\emptyset$ could be chosen to make $W(t)$ show deterministic or stochastic behavior. Berry and Lewis (1980) reported that the deterministic formula including cosine series or alternating sign sine series shows a tendency to increase gradually with time. On the other hand, considering the random characteristic of wind, the stochastic WM function is thus more suitable for simulating fluctuating wind speed time series with the mean equal to zero. Since $W(t)$ is complex, the stochastic real part $R(t)$ adopted in this study can be expressed as

$$R(t) = A \sum_{n(l)=-\infty}^{\infty} \frac{cos(\emptyset(l)) - cos(\gamma^{n(l)}t + \emptyset(l))}{\gamma^{(2-D)\cdot n(l)}} \quad (1 < D < 2, \gamma > 1) \qquad (11)$$

where $\emptyset$ is taken as a set of random numbers ranging from 0 to 2π; A is an amplitude parameter to

https://doi.org/10.5194/wes-2023-91
Preprint. Discussion started: 16 August 2023
© Author(s) 2023. CC BY 4.0 License.

be determined. The parameter γ of the WM function determines the density of the spectrum and the relative phase differences between the spectral modes (Majumdar and Tien, 1990). It is suggested to be 1.08 for the parameter γ in order to provide dense spectral information (Berry and Lewis, 1980). For a given fractal dimension, Eq. (11) provides an efficient way to simulate random time series. More details of simulation will be discussed in Section 2.3.

For this comparison study, a fractal dimension of 1.7, which is the common value for wind speed series reported in the literature (Li et al., 2001; Cui et al., 2022), was applied in Eq. (11) to generate the time series, as shown in Fig. 1. Four estimation methods were then used to estimate the fractal dimension of the generated time series of Fig. 1, and the log-scale fitting plots corresponding to four estimation methods were presented in Fig. 2. Fig. 2 shows that the structure function method provides the most accurate result of 1.6941 with the smallest relative error of 0.35%. By randomly sampling the phase number $\emptyset$ in Eq. (11), 50 different time series have been generated with the same set of parameters (i.e., A=1, D=1.7 and γ=1.08). Fig. 3 presents the estimated results of fractal dimensions for 50 generated time series samples. The structure function method consistently obtained the best estimates around 1.7 compared to other three methods, i.e., box counting method, variation method and R/S analysis method. For a range of fractal dimensions from 1.4 to 1.8, different time series were also generated by Eq. (11), and the fractal dimensions were estimated respectively by four methods and reported in Fig. 4 against the given values. As shown in Fig. 4, the structure function method is the most accurate method to estimate the fractal dimension of a given time series.

https://doi.org/10.5194/wes-2023-91
Preprint. Discussion started: 16 August 2023
© Author(s) 2023. CC BY 4.0 License.
eawe european academy of wind energy
Open Access WIND ENERGY SCIENCE DISCUSSIONS

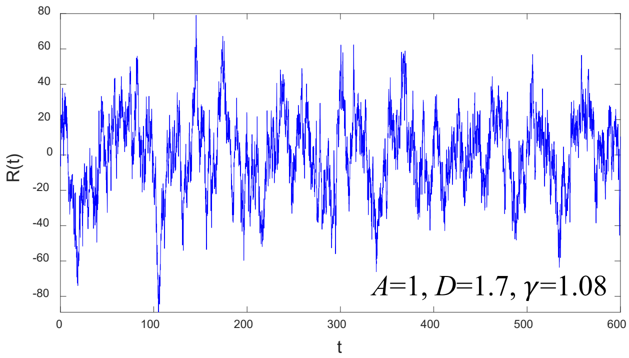

Fig. 1 The generated stochastic function time series

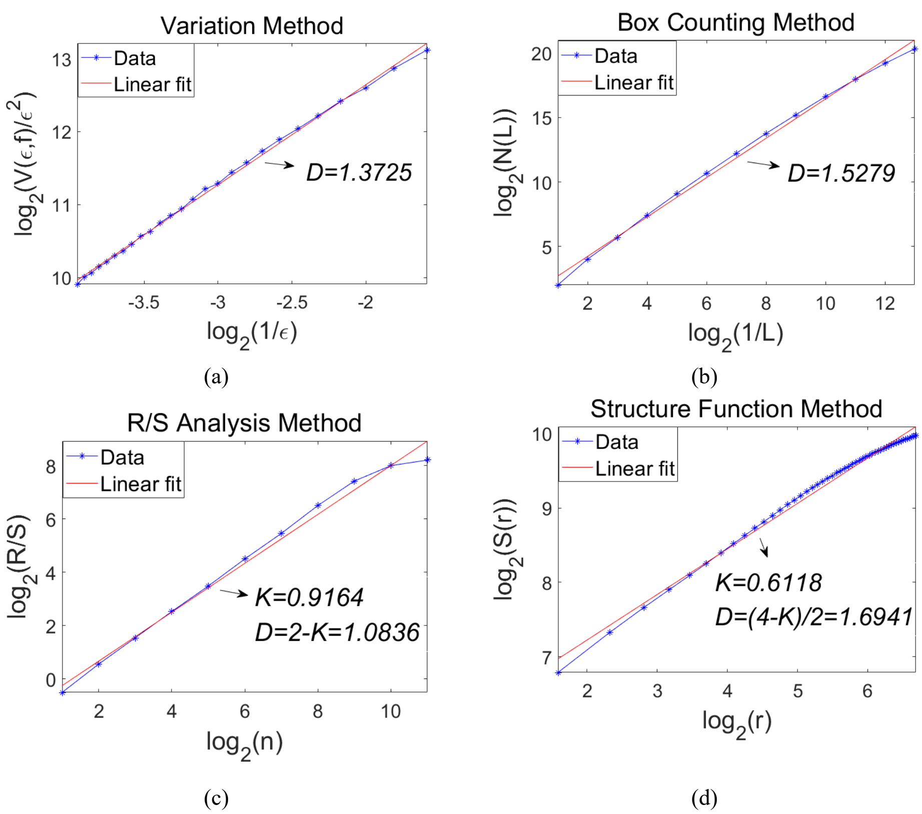

Fig. 2 Log-scale fitting plots corresponding to four fractal dimension estimation methods

https://doi.org/10.5194/wes-2023-91
Preprint. Discussion started: 16 August 2023
© Author(s) 2023. CC BY 4.0 License.

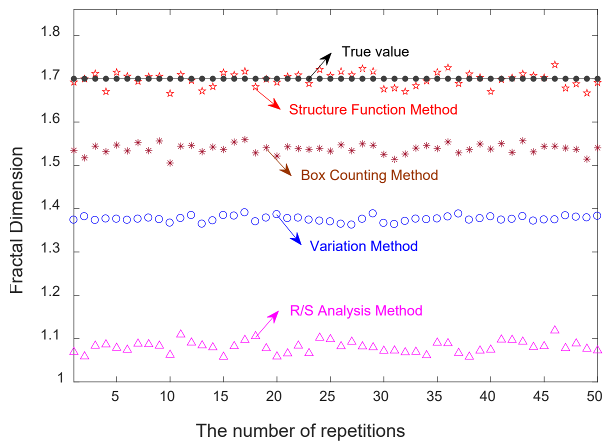

Fig. 3 Estimation results of fractal dimensions for 50 generated time series samples

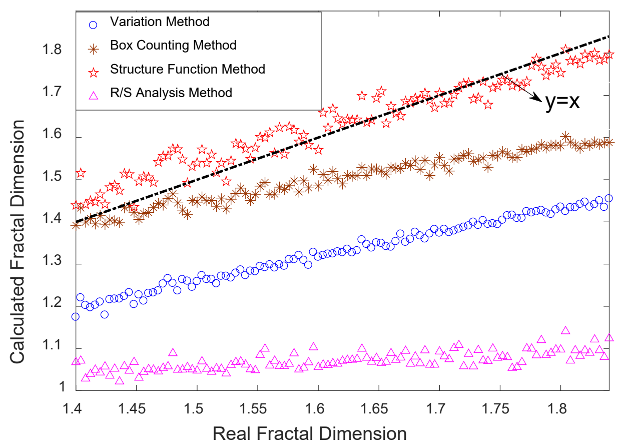

Fig. 4 The estimated fractal dimensions with the actual value

2.2 Time-varying mean of a non-stationary time series

In extreme wind environments, such as tropical cyclones, thunderstorms, downbursts, and strong winds, the wind speed history exhibits significant non-stationary characteristics (Gurley and Kareem, 1997; Wood et al., 2001; Pinelli et al., 2004; Jung and Masters, 2013; Solari et al., 2015). Therefore, the associated overall wind speed series in these environments need to be considered as the sum of the time-varying mean (TVM) component (i.e., non-fractal component, reflecting the non-stationarity of

https://doi.org/10.5194/wes-2023-91
Preprint. Discussion started: 16 August 2023
© Author(s) 2023. CC BY 4.0 License.

the extreme wind speed field) and the fluctuating component (fractal component). Additionally, the adopted WM function $R(t)$ is a zero-mean Gaussian random function because it is the sum of infinite terms with random phases (Guariglia, 2017). Therefore, for simulation of non-stationary wind speeds, the TVM of the overall wind speed time series should be firstly determined by an appropriate method. It is desirable that the de-trended wind speed fluctuation components remain zero-mean over the entire length of the time series.

Cai et al. (2022) proposed a wavelet transform-based method for determining the TVM of non-stationary wind speed series. The measured wind speed time series $U(t)$ can be decomposed as the sum of several detail functions $D_j(t)$ and the approximation function $AF(t)$ (Cai et al. 2022)

$$U(t) = \sum_{j=1}^{M} D_j(t) + AF(t) \tag{12}$$

where M represents the total number of decomposition levels. A series of TVMs of $U(t)$ can be characterized as the superimposition of the approximation function $AF(t)$ and N (non-negative integer) detail functions $D_j(t)$ of the original wind speed series as

$$TVM_N = \begin{cases} AF(t), \quad N = 0 \\ \sum_{j=M+1-N}^{M} D_j(t) + AF(t), \quad 1 \leq N \leq M-1 \end{cases} \tag{13}$$

Subsequently, the relative fluctuating component $u(t)$ of the original wind speed $U(t)$ can be obtained by subtracting the derived TVMs from the original wind speed series, as follows

$$u(t) = \sum_{i=1}^{M-N} D_i(t) \tag{14}$$

According to conditions proposed by Cai et al (2021a, 2021b), the optimal TVM for a wind speed series with a 10-minute time interval has adequate local maxima points but less than six. For better

https://doi.org/10.5194/wes-2023-91
Preprint. Discussion started: 16 August 2023
© Author(s) 2023. CC BY 4.0 License.

characterizing natural wind, stationary or nonstationary wind models could be classified based on the use of constant mean wind speed or the TVM in decomposing wind speed data (Cai et al. 2022).

2.3 Univariate simulation of fluctuating wind speeds

For practice, numerical implementation of Eq. (11) with finite terms can be approximated as

$$R(t) = A \sum_{l=l_{min}}^{l_{max}} \frac{cos\big(\emptyset(l)\big) - \cos\left(\gamma^{n(l)} t + \emptyset(l)\right)}{\gamma^{(2-D)\cdot n(l)}} \quad (\gamma^{n(l_{min})} = 2\pi f_{min}, \gamma^{n(l_{max})} = 2\pi f_{max}) \tag{15}$$

where n_{min} and n_{max} could be determined by the minimum and maximum cut-off frequencies of the fluctuating wind speed spectrum, respectively. According to Cai et al. (2021a, 2021b), the main frequency of optimal TVM is slightly below 0.01Hz. Thus, n_{min} could be approximated as $n(l_{min}) = \ln(2\pi f_{min})/\ln\gamma = -35.96$. For wind engineering practice, a sampling frequency of 10 Hz is normally adopted for full-scale measurements and numerical simulation of turbulent wind. Due to Nyquist-Shannon sampling theorem, the maximum cut-off frequency of the wind speed signal is 5 Hz. Consequently, $n(l_{max})$ could be estimated as $\ln(2\pi f_{max})/\ln\gamma = 44.79$.

For the stochastic WM function $W(t)$, its time-average correlation $\langle|W(t+\tau)W^*(t)|\rangle_t$ is

$$\langle W(t+\tau)W^*(t)\rangle_t = \lim_{T\to\infty} \frac{1}{2T}\int_{-T}^{T} W(t+\tau)W^*(t)dt \tag{16}$$

The power spectrum $S(\omega)$ is proportional to the Fourier transform of the $\langle|W(t+\tau)W^*(t)|\rangle_t$, and is presented, apart from a zero-frequency term, by

$$S(\omega) = \sum_{n(l)=-\infty}^{\infty} \frac{\delta(\omega - \gamma^{n(l)})}{\gamma^{(4-2D)\cdot n(l)}} \tag{17}$$

After averaging discrete spectrum $S(\omega)$ over a range $\Delta\omega$ including Δn frequencies γ^n, a continuous spectrum $\hat{S}(\omega)$ of the stochastic WM function can be obtained as

$$\hat{S}(\omega) = \frac{1}{\Delta\omega}\int_{-\frac{1}{2}\Delta\omega}^{\frac{1}{2}\Delta\omega} S(\omega+\omega')d\omega' \approx \frac{\Delta n}{\Delta\omega\gamma^{(4-2D)\cdot n_\omega}}, \tag{18}$$

https://doi.org/10.5194/wes-2023-91
Preprint. Discussion started: 16 August 2023
© Author(s) 2023. CC BY 4.0 License.

225 where $n_\omega = \frac{\ln(\omega)}{\ln(\gamma)}$. This leads to $\frac{dn_\omega}{d\omega} = \frac{1}{\omega \cdot \ln(\gamma)}$, so that

$$\hat{S}(\omega) \approx \frac{dn_\omega / d\omega}{\gamma^{(4-2D)\cdot n_\omega}} = \frac{1}{ln\gamma \cdot (\omega)^{5-2D}} \tag{19}$$

226 The detailed derivation process is available in Berry and Lewis (1980). When the spectrum is inferred
227 in the Hertz instead of the radian ω of Eq. (19), associated continuous Weierstrass spectrum $\hat{S}(f)$ is
228 given as follows

$$\hat{S}(f) \approx \frac{2\pi}{ln\gamma \cdot (2\pi f)^{5-2D}} \tag{20}$$

229 . As a result, the continuous Weierstrass spectrum $S_R(f)$ of the adopted stochastic real part of $W(t)$,
230 presented in Eq. (15), is approximately estimated as

$$S_R(f) = A^2 \hat{S}(f) \approx \frac{2\pi \cdot A^2}{ln\gamma (2\pi f)^{5-2D}} \tag{21}$$

231 Additionally, a general expression of the wind spectrum $S_u(f)$, given by Olesen et al (1984), was
232 employed as the target spectrum of wind field simulation, as follows

$$\frac{f S_u(f)}{u_*^2} = \frac{a {f_n}^e}{(1 + b f_n^c)^d} \quad (f_n = \frac{fz}{\bar{U}}) \tag{22}$$

233 Where $\bar{U}$ denotes the 10-min mean wind speeds; z is the height of the simulation point; u_* is the
234 friction velocity; a, b, c, d and e are constants, depending on the atmospheric conditions. A
235 coefficient $g(A)$ is newly defined to quantify the difference between the simulated wind spectrum
236 and target spectrum of the fluctuating wind component, given by

$$g(A) = \sum_f (S_R(f) - S_u(f))^2 \tag{23}$$

237 After calculating the derivative of $g(A)$ with respect to A^2, Eq. (24) can be directly obtained.

$$\frac{\partial}{\partial(A^2)} g(A) = \sum_f 2\left(A^2 \hat{S}(f) - S_u(f)\right) \hat{S}(f) \tag{24}$$

238 By taking $\frac{\partial}{\partial(A^2)} g(A) = 0$, the amplitude parameter A is computed as

https://doi.org/10.5194/wes-2023-91
Preprint. Discussion started: 16 August 2023
© Author(s) 2023. CC BY 4.0 License.

$$A = \sqrt{\frac{\sum_f S_u(f) \cdot \hat{S}(f)}{\sum_f (\hat{S}(f))^2}} \tag{25}$$

Then the univariate fluctuating wind speed time histories can be simulated by Eq. (15).

2.4 Multivariate synchronous simulation of wind speeds

Unlike the univariate wind speed simulation, the spatial correlations of wind velocity field should be accounted for the multivariate synchronous simulation of wind speeds (Huang et al, 2020). For this purpose, a following novel way was developed.

The commonly used cross-correlation coefficient to evaluate the correlation of synchronous wind speed time histories (i.e., $X_j(t)$ and $X_k(t)$) at two measured points (P_j and P_k) was given by

$$\rho_{jk} = \frac{E\{[X_j(t) - m_j(t)][X_k(t) - m_k(t)]\}}{\sqrt{E\left\{[X_j(t) - m_j(t)]^2\right\} E\{[X_k(t) - m_k(t)]^2\}}} \tag{26}$$

where $m_j(t)$ and $m_k(t)$ denote the constant means or TVM of wind speed time histories.

Assume that the univariate simulation of fluctuating wind speeds has been implemented by Eq. (15) at the first point P_j, and corresponding phase parameter $\emptyset_j$ has been temporarily stored. At this situation, the synchronous simulation at the second point P_k can be carried out by introducing a Gaussian random sequence φ with zero mean and standard deviation of σ_φ (i.e., $\varphi \sim N(0, {\sigma_\varphi}^2)$) in Eq. (15), as follows

$$R_k(t) = A_k \sum_{l=l_{min}}^{l_{max}} \frac{cos\big(\emptyset_j(l) + \varphi(l)\big) - cos(\gamma^n t + \emptyset_j(l) + \varphi(l))}{\gamma^{(2-D_k)\cdot n(l)}} \tag{27}$$

where A_k is the amplitude parameter estimated by Eq. (15); D_k is the fractal dimension of wind speed series at the second point P_k. The value of $(\emptyset_j + \varphi)$ was converted to $[0 \;\; 2\pi]$ by applying the expression $\emptyset_j + \varphi - 2\pi \cdot floor(\frac{\emptyset_j + \varphi}{2\pi})$, where $floor(x)$ devotes the floor function and returns the greatest integer less than or equal to *x*. If the standard deviation parameter σ_φ of Gaussian distribution

https://doi.org/10.5194/wes-2023-91
Preprint. Discussion started: 16 August 2023
© Author(s) 2023. CC BY 4.0 License.

approaches zero, the phase difference between $(\emptyset_j+\varphi)$ and $(\emptyset_j)$ becomes negligible, resulting in a perfect correlation between simulated fluctuating speed time histories at points (P_j and P_k) by using Eq. (15) and Eq. (27), respectively. Consequently, their cross-correlation coefficient ρ_{jk} computed using Eq. (26) approaches the unity. Additionally, as σ_φ increases, the larger phase difference φ weakens their correlation, leading to a smaller ρ_{jk} until they become irrelevant. To investigate this relationship, 10000 samples of σ_φ were taken from 0 to π, and corresponding variation of ρ_{jk} with the standard deviation parameter σ_φ was plotted in Fig. 5. The figure clearly shows a decreasing trend of ρ_{jk} with increasing σ_φ, and a fitted expression is provided as

$$\rho=\frac{1}{\pi}\arctan\left(-\frac{7}{6}\alpha^3-\frac{1}{8}\alpha^2-\frac{5}{4}\alpha+\frac{9}{25}\right)+\frac{1}{2}\quad(\alpha=log_2(\sigma_\varphi))\tag{28}$$

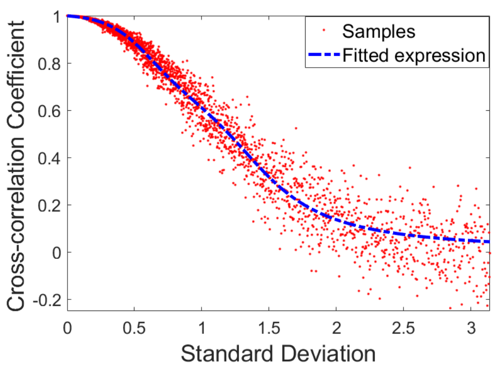

Fig. 5 The variation of cross-correlation coefficient ρ_{jk} with the standard deviation parameter σ_φ

It is easy to obtain that the value of ρ in Eq. (28) falls between 0 and 1, and decrease with the increase of σ_φ after proving $\partial\rho/\partial\alpha<0$. So far, once the synchronous wind speed data was measured at two different spatial points P_k and P_j, ρ_{jk} can be easily calculated using Eq. (26). The corresponding unique value of σ_φ can then be determined by taking the inverse of Eq. (28), enabling the implementation of multivariate wind velocity field simulation using Eq. (15) and Eq. (27). It should be noted that if the estimated correlation of ρ_{jk} for the measured wind speed data sample is negative,

https://doi.org/10.5194/wes-2023-91
Preprint. Discussion started: 16 August 2023
© Author(s) 2023. CC BY 4.0 License.

the expression of fluctuating wind speed in Eq. (27) could be modified by adding the phase π in Eq. (27), as follows

$$R_k(t) = A_k \sum_{l=l_{min}}^{l_{max}} \frac{cos\big(\emptyset_j(l) + \varphi(l) + \pi\big) - cos(\gamma^{n(l)}t + \emptyset_j(l) + \varphi(l) + \pi)}{\gamma^{(2-D_k)\cdot n(l)}} \tag{29}$$

where the associated standard deviation σ_φ of Gaussian distribution φ was derived by taking the inverse of Eq. (28) as $\rho = -\rho_{jk}$ was set.

It is worth noting that if measured wind speed data is not available, the classical spectra known as the Davenport spectrum (Davenport, 2010), von Karman spectrum (Von Karman, 1948), Simiu spectrum (Simiu and Scanlan, 1996), or Harris spectrum (Harris, 1968) can be considered as the target spectrum in Eq. (22). In such situation, the mean fractal dimension D=1.75 estimated by the structure function method in the following section 3.2 is suggested for use in Eq. (15), Eq. (27), and Eq. (29) to simulate the wind speed field.

The detailed multivariate synchronous simulation of wind speed time histories in this paper mainly includes the following steps, as shown in Fig. 6.

Step 1. To check the stationarity of the wind speed sample using the run test (Rouillard, 2014). Subtract the constant mean component to obtain the fluctuating wind speed for stationary data, and subtract the time-varying mean component for non-stationary sample.

Step 2. To estimate each fractal dimension D (D_k and D_j) of fluctuating wind speeds at two different points (P_k and P_j) by using the structure function method.

Step 3. To derive the desired target spectrum $S_u(f)$ based on the measured wind speed data, and determine the parameter A (A_k and A_j) by Eq. (25).

Step 4. To simulate the fluctuating wind speed at reference point P_j by Eq. (15), and record the

https://doi.org/10.5194/wes-2023-91
Preprint. Discussion started: 16 August 2023
© Author(s) 2023. CC BY 4.0 License.

phase parameter $\emptyset_j$ at this step.

Step 5. To evaluate the cross-correlation coefficient ρ_{jk} of measured fluctuating wind speeds at two points P_k and P_j; determine the standard deviation σ_φ using the inverse of Eq. (28); generate a Gaussian random sequence $\varphi \sim N(0, {\sigma_\varphi}^2)$, and then simulate synchronous fluctuating wind speed time series at the point P_k by Eq. (27) for $\rho_{jk} < 0$ or Eq. (29) for $\rho_{jk} > 0$.

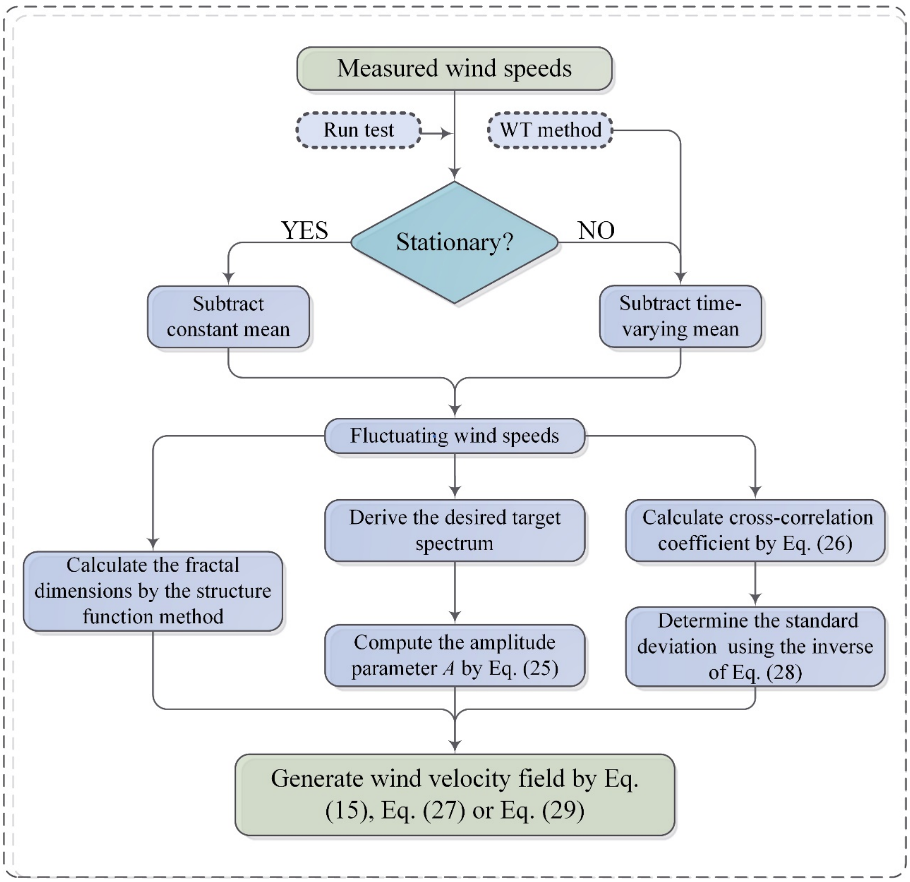

Fig. 6 Flowchart of the multivariate synchronous simulation of wind speeds

3 Results and discussions

3.1 Data source and description

https://doi.org/10.5194/wes-2023-91
Preprint. Discussion started: 16 August 2023
© Author(s) 2023. CC BY 4.0 License.

The wind speed data in this study were continuously recorded by four three-dimensional (3D) sonic anemometers during the occurrence of super typhoon Mangkhut from September 15 to September 18, 2018. The recorded data consists of 526 consecutive 10-minute wind speed samples, with an accuracy of ±0.1 m/s. Four sonic anemometers were installed at the meteorological gradient tower with a height of 356 m in Shenzhen, China (22°38’59’’N, 113°53’36’’E), as shown in Fig. 7. The technical parameters of the sonic anemometers and their install heights are detailed in Table 1.

Typhoon Mangkhut initiated as a tropical depression at 12°N, 170°E and ultimately made landfall over Guangdong, China, on September 16, before moving inland. The associated typhoon track is presented in Fig. 7. The means of longitudinal wind speed data with a fixed period of 10 min during the passage of Mangkhut were recorded at length, as shown in Fig. 8. It is evident that the mean wind speed increases gradually with the increase of recorded heights. Maximum wind speeds were synchronously recorded for four anemometers around 14:00, on September 16, with a maximum of 35 m/s at the height of 320 m.

Table 1 Key parameters of the sonic anemometers.

Instrument	Measured height	Observation content	Sampling frequency	Measured range	Accuracy
CSAT3 3D sonic anemometers	10 m, 40 m,160 m, and 320 m above the ground level	Three directional wind components and sonic virtual temperature	10Hz	0-75 m/s	±0.1 m/s

https://doi.org/10.5194/wes-2023-91
Preprint. Discussion started: 16 August 2023
© Author(s) 2023. CC BY 4.0 License.

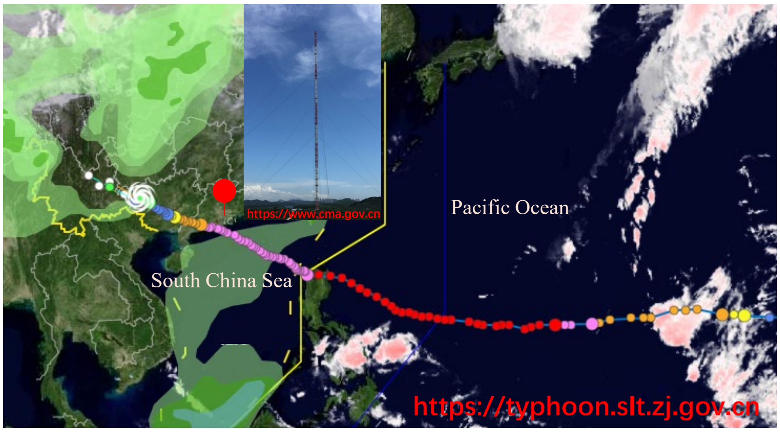

Fig. 7 The location and ambient terrain of the meteorological gradient tower and the track of typhoon Mangkhut

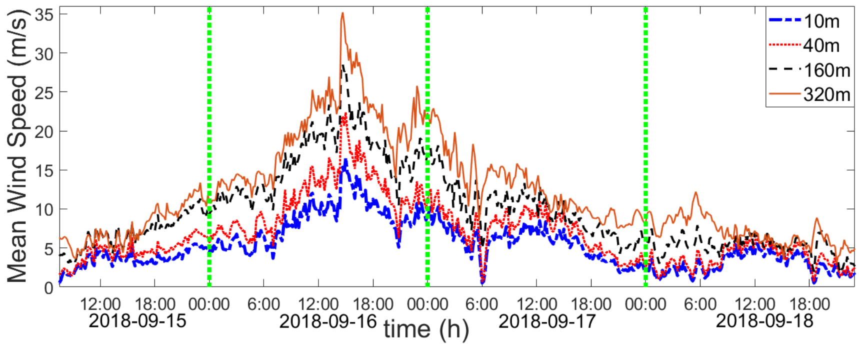

Fig. 8 10-min longitudinal mean wind speeds at each height

3.2 Analysis of fractal dimensions

The fractal dimensions of the longitudinal fluctuating wind speed data during super typhoon Mangkhut were estimated for both stationary and nonstationary wind models. Fig. 9 shows the variation of the relative frequency value (RF-value) of obtained fractal dimensions, where the numbers marked on the X axis are middle values of segment intervals. Furthermore, the difference values (D-value) between corresponding RF-values utilizing stationary and nonstationary wind models lie in the bottom line of each subgraph in Fig. 9. The zoom-in views of bottom graphs in the Fig. 9(a) and Fig. 9(d) are respectively presented in the interval of [-0.02 0.02] and [-0.04 0.04] to provide a more detailed view. As shown in Fig. 9(a) and (d), the results of estimated fractal dimension seem no obvious

© Author(s) 2023. CC BY 4.0 License.

difference between stationary and nonstationary wind models when applying variation method or structure function method. On the other hand, if box counting method or R/S analysis method is used, significant difference of estimated fractal dimension could be observed between stationary and nonstationary models, as shown in Fig. 9(b) and (c). Relevant statistical parameters including mean, standard deviation, maximum and minimum values of fractal dimensions are given in Table 2. Fig. 10 presents the mean fractal dimensions by averaging results corresponding to four measurement heights. Additionally, fractal dimension estimations using the same types of methods by other researchers are reported in Table 3 for further comparison.

According to the findings presented in Fig. 9, there are notable discrepancies in the fractal dimensions obtained from different methods. The variation method yielded a smaller fractal dimension than the box counting method for the same Typhoon wind speed data depicted in Fig. 9(a) and Fig. 9(b). Its main concentration range of the fractal dimension is from 1.354 to 1.502, accounting for more than 90%, and smaller than those calculated by Syu and Kirchhoff (1993) and Li et al (2001) for the normal wind in Table 3 when the same variation method was adopted.

In the case of the box counting method, the mean fractal dimension of winds measured at four heights of 10, 40, 160, and 320 m (i.e., 1.5296, 1.5412, 1.5351 and 1.5423) in Table 2 are close to the values of seasonal monsoon reported by Shu et al. (2021) (i.e., 1.582, 1.570, 1.554 and 1.547) collected from the same meteorological gradient tower. The fractal dimension estimated by the box counting method for typhoon Mangkhut is ranged from 1.4026 to 1.6597, which are similar to the results given by Chang et al (2012), Shu et al (2020), Yan et al (2020) and Cui et al (2022) as reported in Table 3.

For the R/S analysis method, it produced a minimum estimate close to 1, as depicted in Fig. 9(c)

https://doi.org/10.5194/wes-2023-91
Preprint. Discussion started: 16 August 2023
© Author(s) 2023. CC BY 4.0 License.

and Table 2. Although the fractal dimension obtained in this study was comparable to those reported by Tsekouras and Koutsoyiannis (2014) and Balkissoon et al. (2020), it was far lower than the values suggested by most of researchers in Table 3. Furthermore, since the extraction of TVM of nonstationary wind speeds greatly affects the dimension D obtained by the R/S analysis method from Fig. 9(c) and Fig. 10(c), it is not a reliable approach for determining fractal dimensions of wind speed series.

Regarding the structure function method, it yielded the mean fractal dimension of 1.7512 close to the representative value of 1.7. Additionally, the estimated fractal dimension by the structure function method is quite robust and insensitive to stationary or nonstationary wind models used. Therefore, it is reasonable to recommend the structure function method as the effective and reliable approach for estimating the fractal dimension of wind speed series.

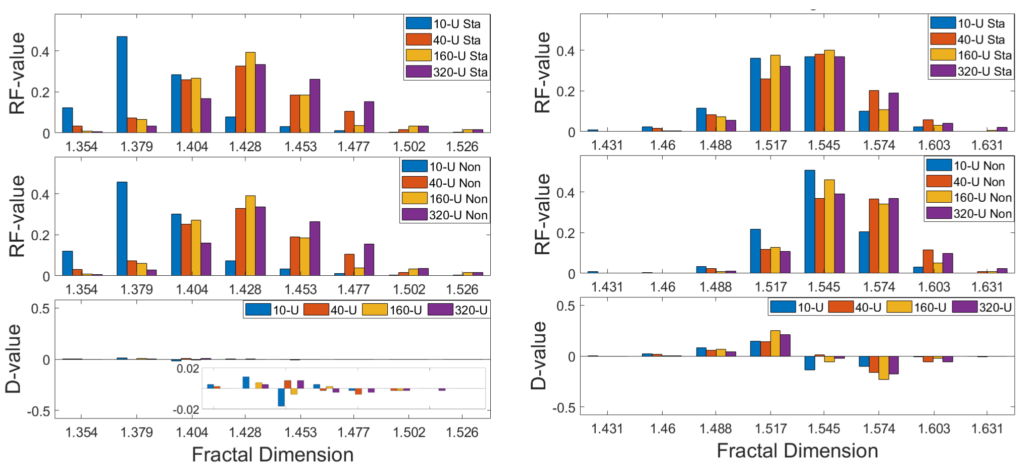

(a) Variation Method (b) Box Counting Method

https://doi.org/10.5194/wes-2023-91
Preprint. Discussion started: 16 August 2023
© Author(s) 2023. CC BY 4.0 License.
WIND ENERGY SCIENCE DISCUSSIONS

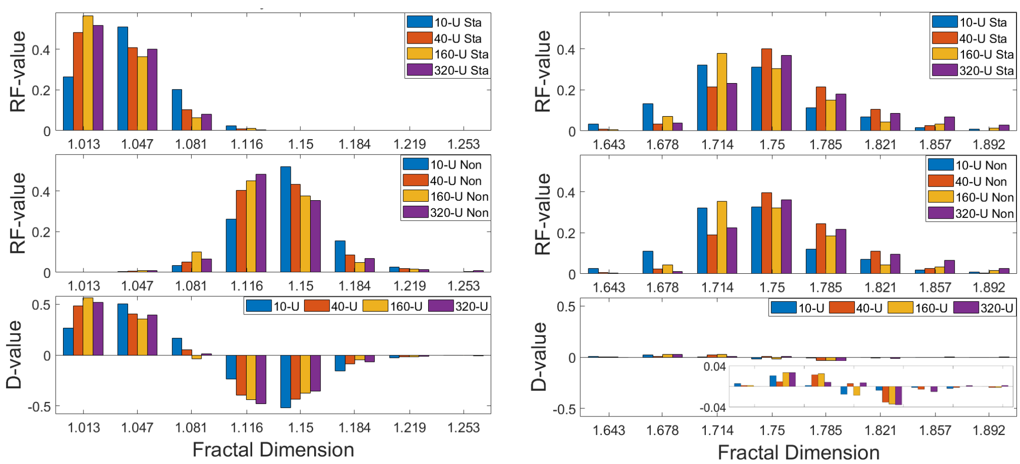

(c) R/S Analysis Method (d) Structure Function Method

Fig. 9 Relative frequency value of fractal dimensions of fluctuating wind speed samples at each measured height based on stationary and nonstationary wind models (Note: Sta: Stationary, Non: Nonstationary)

Table 2 Statistical summary of fractal dimensions of 526 10-min wind speed samples at each measured height in longitudinal wind directions based on the stationary and nonstationary wind model

Measured height		10 m (Sta/Non)	40 m (Sta/Non)	160 m (Sta/Non)	320 m (Sta/Non)
Structure Function Method	Mean	1.7374/1.7409	1.7575/1.7621	1.7453/1.7505	1.7647/1.7695
	Std	0.0461/0.0452	0.0405/0.0397	0.0469/0.0459	0.0516/0.0506
	Max	1.8800/1.8820	1.8730/1.8760	1.9100/1.9120	1.9270/1.9280
	Min	1.6069/1.6128	1.6316/1.6352	1.6470/1.6532	1.6723/1.6822
Box Counting Method	Mean	1.5296/1.5431	1.5412/1.5584	1.5351/1.5544	1.5423/1.5597
	Std	0.0289/0.0252	0.0298/0.0264	0.0256/0.0224	0.0288/0.0267
	Max	1.6068/1.6113	1.6180/1.6284	1.6334/1.6370	1.6372/1.6597
	Min	1.4137/1.4026	1.4466/1.4447	1.4704/1.4523	1.4514/1.4571
Variation Method	Mean	1.3907/1.3911	1.4272/1.4276	1.4278/1.4284	1.4401/1.4406
	Std	0.0246/0.0245	0.0308/0.0307	0.0292/0.0290	0.0299/0.0297
	Max	1.4940/1.4944	1.5428/1.5429	1.5356/1.5358	1.5508/1.5510
	Min	1.3299/1.3305	1.3458/1.3464	1.3430/1.3435	1.3564/1.3576
R/S Analysis Method	Mean	1.0474/1.1460	1.0342/1.1363	1.0306/1.1305	1.0327/1.1322
	Std	0.0239/0.0273	0.0228/0.0271	0.0231/0.0276	0.0228/0.0288
	Max	1.1162/1.2368	1.1177/1.2873	1.1308/1.2855	1.1217/1.2870
	Min	0.9942/1.0488	0.9784/1.0367	0.9899/1.0565	0.9822/1.0593

https://doi.org/10.5194/wes-2023-91
Preprint. Discussion started: 16 August 2023
© Author(s) 2023. CC BY 4.0 License.

367 Table 3 The fractal dimension estimation result for the wind speed data from different references

References	Applied method	Details about obtained fractal dimension	Type of wind
Syu and Kirchhoff (1993)	variation method	*D*=1.60±0.03 for six different wind speed records from Altamont taken on different days	Normal wind
Li et al (2001)	variation method	average about 1.70	Normal wind
This study	variation method	Vary from 1.3299 to 1.5510	Typhoon wind
Barszcz et al (2012)	box counting method	mean fractal dimension of 1.3552 for the fluctuating wind speed	Normal wind
Chang et al (2012)	box counting method	Annual mean fractal dimension values ranging from 1.61 to 1.66	Normal wind
Tijera et al (2012)	box counting method	Fractal dimensions of 1.30 to nearly 1.00 for the 5-min horizontal and vertical velocity fluctuations	Normal wind
Fortuna et al (2014)	box counting method	*D*=1.19 for daily mean wind speeds *D*=1.41 for hourly mean wind speeds	Normal wind
Wu et al. (2015)	box counting method	*D*=1.46, 1.35 and 1.24 for the 10-min fluctuating wind speed at the measured height of 3.5 m, 6.5 m and 10 m, respectively.	Normal wind
Shu et al (2020)	box counting method	Mean fractal dimension varying from 1.31 at an offshore weather station to 1.43 at an urban station	Normal wind
Yan et al (2020)	box counting method	Daily fractal dimensions of 10-min wind speed time series estimated between 1.32 and 1.47 based on 6-year continuous anemometric data	Normal wind
Shu et al (2021)	box counting method	*D*=1.582, 1.570, 1.554, and 1.547 for the 10-min vertical wind velocity of seasonal monsoon at the measured heights of 10, 40, 160, and 320 m, respectively.	Normal wind
Cui et al (2022)	box counting method	*D* varied from 1.55 to 1.75 for the measured 10-min horizontal wind speeds during the three typhoons landing (Typhoon Lionrock, Fanapi and Megi)	Typhoon wind
This study	box counting method	Vary from 1.4026 to 1.6597	Typhoon wind
Tsekouras and Koutsoyiannis (2014)	R/S analysis method	The majority of the *D* of wind speeds lying in the interval (1.1, 1.4)	Normal wind
Balkissoon et al (2020)	R/S analysis method	The fractal dimensions varying from 1.1 to 1.3 for the monthly wind speed time series.	Normal wind
This study	R/S analysis method	Vary from 0.9784 to 1.2873	Typhoon wind
This study	Structure Function Method	Vary from 1.6069 to 1.9280	Typhoon wind

368

https://doi.org/10.5194/wes-2023-91
Preprint. Discussion started: 16 August 2023
© Author(s) 2023. CC BY 4.0 License.

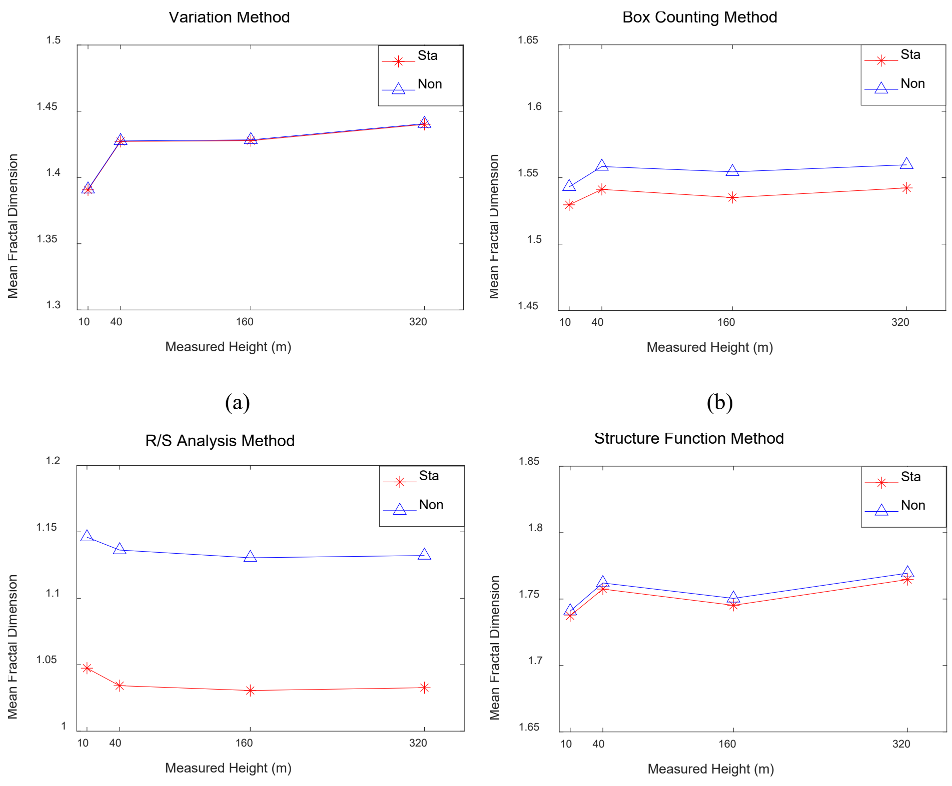

(a) (b) (c) (d)

Fig. 10 Mean fractal dimensions under stationary and nonstationary wind models

3.3 Simulation of fluctuating wind speeds

Fluctuating wind speeds at two heights of 160 m and 320 m were simulated based on two synchronously measured records. The optimal TVMs extracted by the wavelet transform-based method in section 2.2 are presented in Fig. 11 after determining that these two wind speed samples were non-stationary based on the run test method.

As for the fluctuating wind speed at the height of 320 m, the fractal dimension D=1.7427 was estimated by structure function method, and corresponding least-square fit result of the curve $\log_2(S(r))$ with $\log_2(r)$ was presented in Fig. 12(a). After getting the fitted target spectrum $S_u(f)$ and calculating the amplitude parameter A=0.0520 by Eq. (25), the wind speed time series were then simulated using

https://doi.org/10.5194/wes-2023-91
Preprint. Discussion started: 16 August 2023
© Author(s) 2023. CC BY 4.0 License.

Eq. (15), as illustrated in Fig. 13 and Fig.14. The fractal dimension of the simulated wind speed time series was determined using the structure function method, yielding a value of D=1.7163, as depicted in Fig. 12(b). These results indicate that the simulated wind speeds exhibit similar fractal characteristics with the original wind component. Moreover, the standard deviations of the actual and simulated fluctuating wind speeds were found to be 1.2030 and 1.2125, respectively, with a negligible relative error of 0.79%.

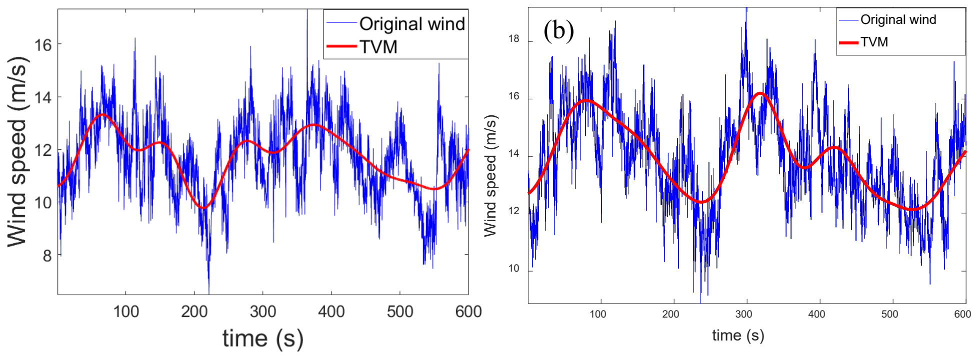

Fig. 11 Measured 10-minute wind speed samples and their TVMs at the height of (a)160 m and (b)320 m

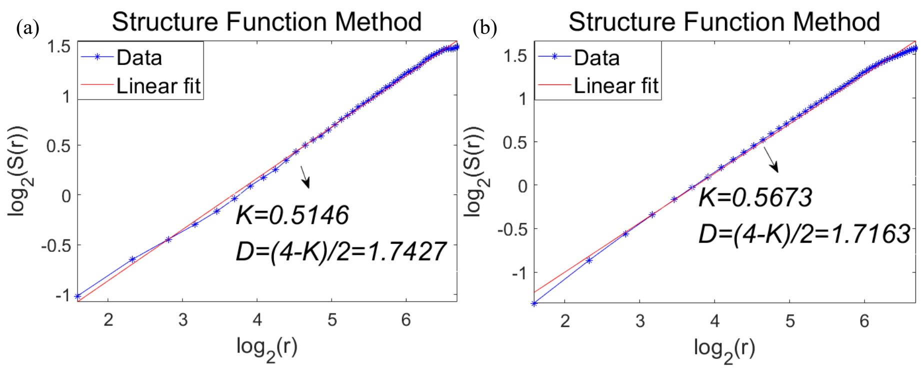

Fig. 12 Plot of $\log_2(S(r))$ versus $\log_2(r)$ and relative least-square fitting result (red line): (a) Original fluctuating wind (b) Simulated fluctuating wind at the height of 320m

Additionally, wind speed time histories were also simulated using the conventional HSM for comparison with the proposed SWM method, as shown in Figs. 13 and 14. Fig. 13(b) demonstrates that the probability density functions of simulated fluctuating wind by the proposed SWM in this study

https://doi.org/10.5194/wes-2023-91
Preprint. Discussion started: 16 August 2023
© Author(s) 2023. CC BY 4.0 License.

and commonly used HSM method are similar to that of the measured wind record, and each probability distribution fits well with the Gaussian distribution. According to Fig. 14, it can be observed that the original wind speed spectrum shows a tendency to deviate from the classical von Karman spectrum beyond a frequency of 2 Hz, which might be attributed to the existence of Gaussian white noise in the measured wind data as reported by Kaimal and Finnigan (1994). Fig. 15 shows the evolutionary power spectral density (EPSD) of nonstationary wind speeds to reveal the turbulent energy distribution both in time and frequency domain (Priestley, 1965). The similarity of wind spectra and EPSDs between the actual and simulated wind in Figs. 14 and 15 provides the strong evidence for the effectiveness of the proposed wind speed simulation method.

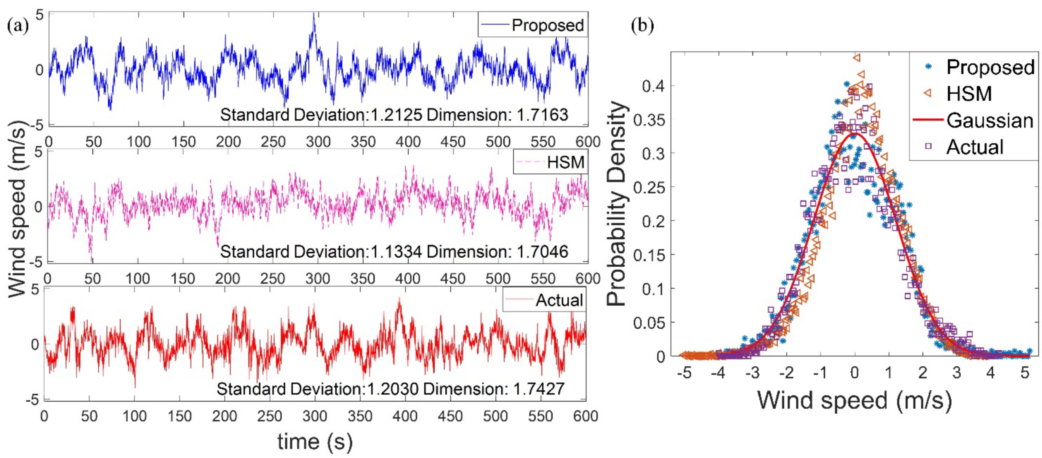

Fig. 13 (a) Simulated and original fluctuating wind speed time series, and (b) corresponding probability density function at the height of 320m

https://doi.org/10.5194/wes-2023-91
Preprint. Discussion started: 16 August 2023
© Author(s) 2023. CC BY 4.0 License.

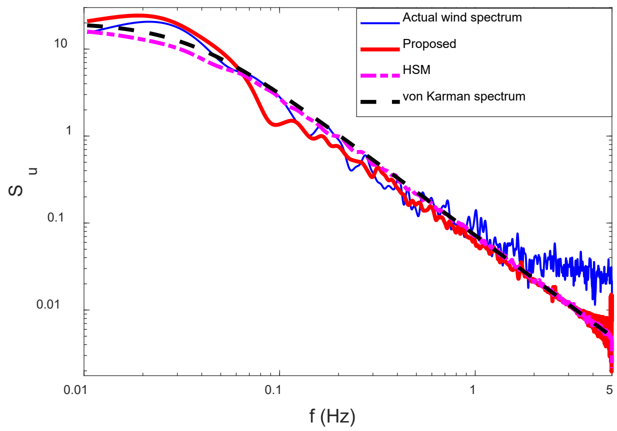

Fig. 14 Wind spectra of the fluctuating wind speeds

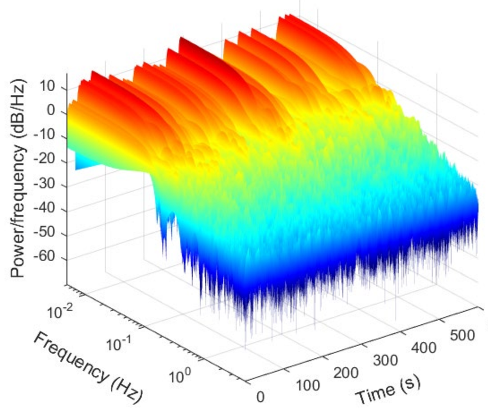

(a) EPSD of the fluctuating wind simulated by SWM

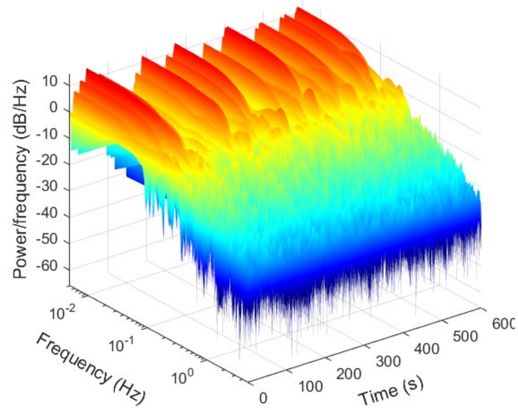

(b) EPSD of the fluctuating wind simulated by HSM

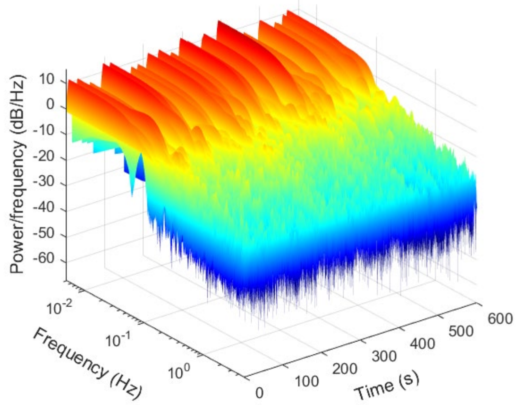

(c) EPSD of the actual fluctuating wind

Fig. 15 Estimated EPSD

https://doi.org/10.5194/wes-2023-91
Preprint. Discussion started: 16 August 2023
© Author(s) 2023. CC BY 4.0 License.

Based on multivariate synchronous measurement at two heights of 160 m and 320 m, the cross-correlation coefficient of two wind speed series in Fig. 11 was calculated by Eq. (26) as $\rho_{jk} = 0.115 > 0$. After the parameter σ_{φ}=2.12 was obtained by taking the inverse of Eq. (28), Eq. (27) could be used to generate fluctuating wind series at the height of 160 m. Fig. 16 shows the simulation results in terms of spectrum and fractal dimension. It was found the proposed SWM method can generate the fluctuating wind series of second variate (at the height of 160 m) with very close properties to the measured wind speed sample, i.e., wind spectrum, standard deviation, fractal dimension and the specified cross-correlation to the first variate (at the height of 320 m).

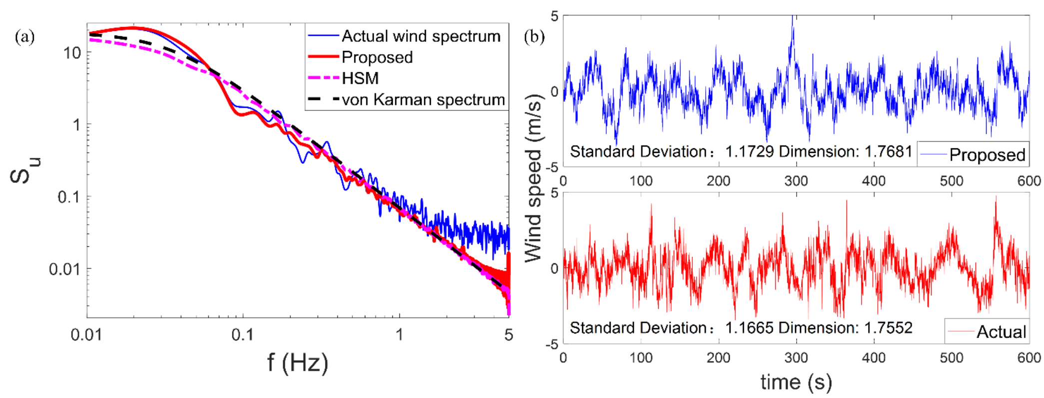

Fig. 16 Simulation result of second variate at the height of 160 m (a) Wind spectra and (b) Fluctuating wind speeds

To further verify the effectiveness of the proposed SWM method, the 22-hour typhoon wind speed samples from 7 am September 15 to 5 am September 16, i.e., 132 10-minute samples measured at two representative heights of 160 m and 320 m were utilized. The 10-minute fluctuating wind series are then recursively generated for the two different heights as time marching with a time step of 10-minute. The fractal dimensions of the real and simulated fluctuating wind components were estimated by the structure function method. Fig. 17 demonstrates that there is almost no difference in fractal dimensions between the real and simulated wind fluctuations of the first variate (at the height of 320 m). For the

https://doi.org/10.5194/wes-2023-91
Preprint. Discussion started: 16 August 2023
© Author(s) 2023. CC BY 4.0 License.

second variate, slight difference of fractal dimension was observed between the real and simulated wind series due to the introduction of the Gaussian random phase variable φ in Eq. (27) or Eq. (29). Fig. 18 shows that the evolution of standard deviation of the simulated wind series by the SWM method, which are in close agreement with those of the real fluctuating winds during 7 am September 15 to 5 am September 16, 2018. By combining the TVM components, the proposed SWM is able to reproduce nonstationary typhoon wind speed series effectively.

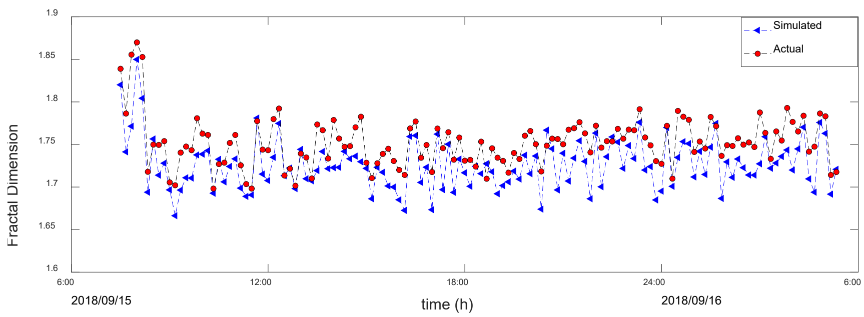

(a) 160 m

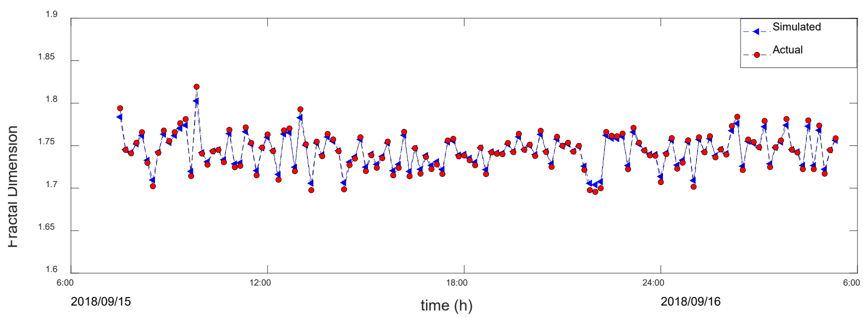

(b) 320 m

Fig. 17 Fractal dimensions of real and simulated fluctuating wind speeds

https://doi.org/10.5194/wes-2023-91
Preprint. Discussion started: 16 August 2023
© Author(s) 2023. CC BY 4.0 License.

eawe european academy of wind energy
Open Access WIND ENERGY SCIENCE DISCUSSIONS

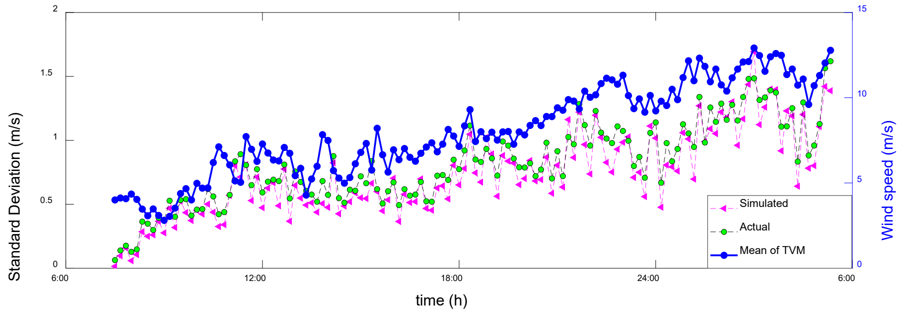

(a) 160 m

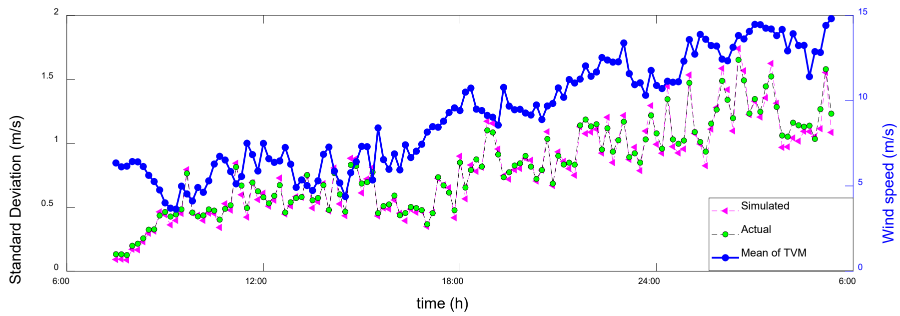

(b) 320 m

Fig. 18 Standard deviation of real and simulated fluctuating wind speeds with the mean of each TVM

4 Conclusions

This paper focuses on determining an appropriate method for the fractal dimension estimation of wind speeds, and then propose the stochastic WM function-based numerical simulation method (SWM method) for the multivariate wind speed simulation. The study shows that the structure function method is a more suitable technique for estimating the fractal dimension than the box counting method, variation method, and R/S analysis method. Field-measured wind data recorded during Typhoon Mangkhut (2018) were used to present the performance of the proposed method. The specific findings are as follows

(1) Various methods to determine the fractal dimension of winds affect the accuracy of the estimated

© Author(s) 2023. CC BY 4.0 License.

fractal dimension estimation. The mean fractal dimension of 1.75 obtained by the structure function method is closest to the representative value of 1.7 than other three methods. Furthermore, the estimated fractal dimension by the structure function method is quite robust and insensitive to stationary or nonstationary wind models used.

(2) The multivariate wind speed components simulated by the proposed fractal-based SWM method are in good agreement with the measured records in terms of fractal dimension, standard deviation, probability density function, wind spectrum and cross-correlation coefficients. The proposed SWM method combined with the TVM components is capable of generating nonstationary multivariate typhoon wind speeds.

Declaration of competing interest

The authors declare that they have no known competing financial interests or personal relationships that could have appeared to influence the work reported in this paper.

Acknowledgments

The work described in this paper was partially supported by the National Natural Science Foundation of China (Grant No. 52178512), and Natural Science Foundation of Zhejiang Province (Grant No. LZ22E080006).

References

Arenas, A., Chorin, A.J. (2006). On the existence and scaling of structure functions in turbulence according to the data. *Proc Natl Acad Sci U S A*, 103(12):4352-5

Balkissoon, S., Fox, N., Lupo, A. (2020). Fractal characteristics of tall tower wind speeds in missouri.

https://doi.org/10.5194/wes-2023-91
Preprint. Discussion started: 16 August 2023
© Author(s) 2023. CC BY 4.0 License.

Renewable Energy, 154: 1346-1356

Barszcz, T., Bielecka, M., Bielecki, A., Wójcik, M. (2012). Wind speed modelling using weierstrass function fitted by a genetic algorithm. *Journal of Wind Engineering and Industrial Aerodynamics*, 109: 68–78

Berry, M.V., Lewis, Z.V. (1980). On the weierstrass-mandelbrot fractal function. *Proceedings of the Royal Society of London*, 370(1743): 459-484.

Breslin, M.C., Belward, J.A. (1999). Fractal dimensions for rainfall time series. *Mathematics and Computers in Simulation*, 48 (4–6): 437–446.

Cadenas, E., Campos-Amezcua, R., Rivera, W., Espinosa-Medina, M.A., Mendez-Gordillo, A.R., Rangel, E., Tena, J. (2019). Wind speed variability study based on the Hurst coefficient and fractal dimensional analysis. *Energy Science and Engineering*, 7(2): 361–378.

Cai, K., Li, X., Zhi, L.H. (2021a). Extracting time-varying mean component of non-stationary winds utilizing vondrak filter and genetic algorithm: a wind engineering perspective. *International Journal of Structural Stability and Dynamics*. 21(11), 2150155.

Cai, K., Li, X., Zhi, L.H., Han, X.L. (2021b). Extraction of optimal time-varying mean of non-stationary wind speeds based on empirical mode decomposition. *Structural Engineering and Mechanics*, 77(3): 355-368

Cai, K., Huang, M.F., Xu, H.W., Kareem, A. (2022). Analysis of Nonstationary Typhoon Winds Based on Optimal Time-Varying Mean Wind Speed. *Journal of Structural Engineering*, 148(12):04022199.

Chang, T.P., Ko, H.H., Liu, F.J., Chen, P.H., Chang, Y.P., Liang, Y.H., Jang, H.Y., Lin, T.C., Chen, Y.H.

https://doi.org/10.5194/wes-2023-91
Preprint. Discussion started: 16 August 2023
© Author(s) 2023. CC BY 4.0 License.

(2012). Fractal dimension of wind speed time series. *Applied Energy*, 93: 742–749.

Chen, K.L., Yu, J. (2014). Short-term wind speed prediction using an unscented Kalman filter based state-space support vector regression approach. *Applied Energy*, 113:690-705.

Cui, B.C., Huang, P., Xie, W. (2022). Fractal dimension characteristics of wind speed time series under typhoon climate. *Journal of Wind Engineering and Industrial Aerodynamics*, 229, 105144.

Davenport, A.G. (2010). The spectrum of horizontal gustiness near the ground in high winds. *Quarterly Journal of the Royal Meteorological Society*, 87(372), 194-211.

Dubuc, B., Roques-Carmes, C., Tricot, C., Zucker, S.W. (1987). The variation method: a technique to estimate the fractal dimension of surfaces. *Proceedings of SPIE - The International Society for Optical Engineering*, 845, 241.

Fortuna, L., Nunnari, S., Guariso, G. (2014). Fractal order evidences in wind speed time series. *International Conference on Fractional Differentiation and its Applications*, 1–6.

Ganti, S., Bhushan, B. (1995). Generalized fractal analysis and its applications to engineering surfaces. *Wear*, 180(1-2): 17-34.

Guariglia, E. (2017). Spectral analysis of the Weierstrass-Mandelbrot function. *IEEE 2nd International Multidisciplinary Conference on Computer and Energy Science-SpliTech2017. IEEE.*

Gurley, K., Kareem, A. (1997). Analysis interpretation modeling and simulation of unsteady wind and pressure data. *Journal of Wind Engineering and Industrial Aerodynamics*, 69–71(1): 657-669.

Harrouni, S. (2013). Long term persistence in daily wind speed series using fractal dimension. *International Journal of Multiphysics*, 7(2): 87-94.

Harrouni, S. (2018). Using fractal dimension to evaluate wind gusts long-term persistence. *2nd*

https://doi.org/10.5194/wes-2023-91
Preprint. Discussion started: 16 August 2023
© Author(s) 2023. CC BY 4.0 License.

European Conference on Electrical Engineering and Computer Science, 416–420.

Harris, R.I. (1968). On the spectrum and autocorrelation function of gustiness in high wind. *ERA Report 5273.*

Higuchi, T. (1988). Approach to an irregular time series on the basis of the fractal theory. *Physica D Nonlinear Phenomena*, 31(2): 277-283.

Huang, G.Q., Peng, L.L., Kareem, A., Song, C.C. (2020). Data-driven simulation of multivariate nonstationary winds: a hybrid multivariate empirical mode decomposition and spectral representation method. *Journal of Wind Engineering and Industrial Aerodynamics*, 197: 104073.

Humphrey, J., Schuler, C.A., Rubinsky, B. (1992). On the use of the weierstrass-mandelbrot function to describe the fractal component of turbulent velocity. *Fluid Dynamics Research*, 9(1-3): 81-95.

Jiang, C., Lu, Z., Jin, Z., Memon, M.S. (2017). Evaluation of fractal dimension of soft terrain surface. *Journal of Terramechanics*, 70: 27-34.

Jung, S., Masters, F.J. (2013). Characterization of open and suburban boundary layer wind turbulence in 2008 hurricane Ike. *Wind and Structures*, 17(2): 135-162.

Kaimal, J.C., Finnigan, J.J. (1994). Atmospheric Boundary Layer Flows: Their Structure and Measurement. New York, USA: Oxford University Press, 304pp.

Li, X., Hu, F., Liu, G., Hong, Z.X. (2001). Multi-scale fractal characteristics of atmospheric boundary-layer turbulence. *Advances in Atmospheric Sciences*, 18(5): 787-792.

Liu, D., Niu, D.X., Wang, H., Fan, L.L. (2014). Short-term wind speed forecasting using wavelet transform and support vector machines optimized by genetic algorithm. *Renewable energy*, 62:

https://doi.org/10.5194/wes-2023-91
Preprint. Discussion started: 16 August 2023
© Author(s) 2023. CC BY 4.0 License.

592–597.

Liu, L., Hu, F., Jun, L., Song, L.L. (2013). On the use of weierstrass-mandelbrot function to simulate fractal wind fluctuations. *Climatic and Environmental Research*, 18(1): 43-50. (In Chinese)

Lyu, R., Hu, F., Liu, L., Cheng, X.L. (2018). Simulation of turbulent wind fluctuations using WAWA-WM method. *Acta Energiae Solaris Sinica*, 39(3): 603-610. (In Chinese)

Majumdar, A., Tien, C.L. (1990). Fractal characterization and simulation of rough surfaces. *Wear*, 136(2): 313-327.

Majumdar, A., Bhushan, B. (1991). Fractal model of elastic-plastic contact between rough surfaces. *J Tribol Trans Asme*, 113(1): 1-11.

Mandelbrot, B. (1983). The Fractal Geometry of Nature. WH Freeman, New York.

Mandelbrot, B. (1994). Fractals-A Geometry of Nature. Exploring Chaos. Norton, New York, pp. 122–135.

Mignoler, P.M., Spanos, P.D. (1987). Recursive simulation of stationary multivariate random processes--Part I. *Journal of Applied Mechanics*, 54: 674-680.

Olaofe, Z.O. (2014). A 5-day wind speed and power forecasts using a layer recurrent neural network (LRNN). *Sustainable Energy Technol Assess*, 6: 1-24.

Olesen, H.R., Larsen, S.E. Højstrup, J. (1984). Modelling velocity spectra in the lower part of the planetary boundary layer. *Boundary-Layer Meteorology*, 29: 285–312.

Rehman, S., Siddiqi, A.H. (2009). Wavelet based Hurst exponent and fractal dimensional analysis of Saudi climatic dynamics. *Chaos, Solitons and Fractals*, 40 (3): 1081–1090.

Peters, E.E. (1991). Chaos and order in the capital markets. *European Company Law*, 1231.

https://doi.org/10.5194/wes-2023-91
Preprint. Discussion started: 16 August 2023
© Author(s) 2023. CC BY 4.0 License.

Pinelli, J.P., Simiu, E., Gurley, K. (2004). Hurricane damage prediction model for residential structures. *Journal of Structural Engineering*. 130(11): 1685-1691.

Rouillard, V. (2014). Quantifying the Non-stationarity of Vehicle Vibrations with the Run Test. *Packaging Technol. Sci*, 27(3): 203-219.

Priestley, M.B. (1965). Evolutionary Spectra and Non-Stationary Processes. *Journal of the Royal Statistical Society*, 27(2): 204-237.

Rubalcaba, J.O. (1997). Fractal analysis of climatic data: annual precipitation records in Spain. *Theoretical and Applied Climatology*, 56 (1–2): 83–87.

Sakamoto, T., Tanizuka, N., Hirata, Y., Aihara, K. (2007). A fractal dimension of wind speed time series. *AIP Conference Proceedings*, 922(1): 709–711.

Sarkar, N., Chaudhuri, B.B. (1994). An efficient differential box-counting approach to compute fractal dimension of image. IEEE Transactions on Systems, Man, and Cybernetics, 24(1): 115-120.

Shinozuka, M., Jan, C.M. (1972). Digital simulation of random processes and its applications. *Journal of Sound and Vibration*, 25(1): 111-128.

Shivamoggi, B. K. (1995). Multi-fractal aspects of the fine-scale structure of temperature fluctuations in isotropic turbulence. *Physica A*, 221(4): 460-477.

Shlesinger, W.M. (1990). The noise in natural phenomena. *American Scientist*, 78(1): 40-45.

Shu, Z.R., Chan, P.W., Li, Q.S., He, Y.C., Yan, B.W., 2020. Quantitative assessment of offshore wind speed variability using fractal analysis. *Wind Struct*, 31, 363–371.

Shu, Z.R., Chan, P.W., Li, Q.S., He, Y.C., Yan, B.W., Li, L., Lu, C., Zhang, L. Yang, H.L. (2021). Characterization of vertical wind velocity variability based on fractal dimension analysis.

https://doi.org/10.5194/wes-2023-91
Preprint. Discussion started: 16 August 2023
© Author(s) 2023. CC BY 4.0 License.

Journal of Wind Engineering and Industrial Aerodynamics, 213(15), 104608.

Simiu, E., Scanlan, R.H. (1996). Wind effects on structures: Fundamentals and applications to design. Wiley, New York.

Solari, G., De Gaetano, P., Repetto, M.P. (2015). Thunderstorm response spectrum: fundamentals and case study. *Journal of Wind Engineering and Industrial Aerodynamics*, 143: 62-77.

Syu, C.Y., Kirchhoff, R.H. (1993). The fractal dimension of the wind. *Journal of Solar Energy Engineering*, 115(3): 151-154.

Tijera, M., Maqueda, G., Yagüe, C., Cano, J.L. (2012). Analysis of Fractal Dimension of the Wind Speed and Its Relationships with Turbulent and Stability Parameters. *Fractal Analysis and Chaos in Geosciences*, 22(2):29-46

Tsekouras, G., Koutsoyiannis, D. (2014). Stochastic analysis and simulation of hydrometeorological processes associated with wind and solar energy. *Renewable Energy*, 63: 624-633.

Thomas, T.R., Rosén, B.G., Amini, N. (1999). Fractal characterisation of the anisotropy of rough surfaces. *Wear*, 232: 41-50.

Von Karman, T. (1948). Progress in the Statistical Theory of Turbulence. *Proceedings of the National Academy of Sciences*, 34(11): 530-539.

Wang, L., Xiang, Y. (2013). A method to determine the fractal roughness parameter from surface profiles generated by the WM function. *Applied Mechanics and Materials*, 341-342(1): 329-332.

Wood, G.S., Kwok, K.C.S., Motteram, N.A., Fletcher, D.F. (2001). Physical and numerical modelling of thunderstorm downbursts. *Journal of Wind Engineering and Industrial Aerodynamics*, 89(6):

535-552.

Wu, H.H., Xu, Y., Hu, L.M., Qin, F.Q., Li, Z.N. (2015). Research on fractal simulation of subsurface fluctuating wind speed time-history. *Earthquake Engineering and Engineering Vibration*, 35(4): 121- 129. (In Chinese)

Yassin, K., Helms, A., Moreno, D., Kassem, H., Höning, L., and Lukassen, L.J. (2023). Applying a random time mapping to Mann-modeled turbulence for the generation of intermittent wind fields, *Wind Energy Science*, 8:1133–1152.

Yan, B.W., Chan, P.W., Li, Q.S., He, Y.C., Shu, Z.R. (2020). Characterising the fractal dimension of wind speed time series under different terrain conditions. *Journal of Wind Engineering and Industrial Aerodynamics*, 201, 104165.

Zhong, L., Zeng, F., Xu, G.X. (2012). Comparison of fractal dimension calculation methods for channel bed profiles. *Procedia Engineering*, 28(5): 252-257.

Zhu, B., Chen, M.Y., Wade, N., Ran, L. (2011). A prediction model for wind farm power generation based on fuzzy modeling. *International Conference on Energy and Environment*, 195–198.